Pakistan Veterinary Journal

ISSN: 0253-8318 (PRINT), 2074-7764 (ONLINE)
DOI: 10.29261/pakvetj/2026.011

RESEARCH ARTICLE

Interferon-Tau Enhances Bovine Endometrial Receptivity Through Dvl3/Rac2 Signaling-Driven Plasma Membrane Transformation During Implantation

Xiaofei Ma*[1,2], Zhonghong Bai[1,2], Tingting Liu[1,2], Saqib Umer[3], Junjie Hu[1,2] and Ganzhen Deng[4]

[1] College of Veterinary Medicine, Gansu Agricultural University, 730070, Lanzhou, Gansu, China; [2] Gansu Key Laboratory of Animal Generational Physiology and Reproductive Regulation, 730070, Lanzhou, Gansu, China; [3] Department of Theriogenology, University of Agriculture, Faisalabad, 38000, Pakistan. [4] Department of Clinical Veterinary Medicine, College of Veterinary Medicine, Huazhong Agricultural University, 430070, Wuhan, Hubei, China.
*Corresponding author: maxf@gsau.edu.cn

ARTICLE HISTORY (25-798)

Received: August 16, 2025
Revised: September 28, 2025
Accepted: October 09, 2025
Published online: January 02, 2026

Key words:
Bovine
Dishevelled segment polarity
Protein 3
Interferon-tau
Plasma membrane
Transformation
Endometrial receptivity

A B S T R A C T

Low endometrial receptivity is the major cause of failure in embryonic implantation and early pregnancy loss in dairy cows. During peri-implantation, bovine endometrial luminal epithelial cells (bELECs) undergo plasma membrane transformation (PMT), the molecular mechanisms of which remain elusive. In this study, we investigated the molecular mechanisms underlying PMT and its role in endometrial receptivity. Analysis of mRNA data from the Gene Expression Omnibus (GEO) database revealed that PMT occurs during the peri-implantation period and is closely associated with the establishment of endometrial receptivity. Interferon-tau (IFN-τ), a pregnancy recognition signal, promoted PMT in bELECs by regulating the dishevelled segment polarity protein 3 (DVL3)/Ras-related C3 botulinum toxin substrate 2 (RAC2) signaling pathway, thereby enhancing endometrial receptivity. IFN-τ upregulated DVL3 and RAC2 expression, facilitating their interaction, which disrupted intercellular connections and enhanced the migration and motility of bELECs. Concurrently, RAC2 accelerated filamentous actin polymerization, further driving PMT. This process increased the expression of PMT and endometrial receptivity markers, suggesting that the DVL3/RAC2 signaling axis, downstream of IFN-τ, could be a potential therapeutic target for rescuing embryo implantation failure caused by abnormal endometrial receptivity in dairy cows.

To Cite This Article: Ma X, Bai Z, Liu T, Saqib U, Hu J and Deng G, 2026. Interferon-tau enhances bovine endometrial receptivity through dvl3/rac2 signaling-driven plasma membrane transformation during implantation. Pak Vet J, 46(1): 21-36. http://dx.doi.org/10.29261/pakvetj/2026.011

INTRODUCTION

Mammalian pregnancy is a complex and delicate process involving fertilization, embryo implantation, placental formation, embryo growth and development, and delivery (Shibata *et al.,* 2024). Early embryo loss owing to implantation failure is a key factor of infertility and a major issue in limiting the development of assisted reproductive technologies (Baron *et al.,* 2021; Schmiech *et al.,* 2025). In high-yielding dairy cows, approximately 50% embryos do not survive even 7 days after insemination, and only ≤ 30% of these cows calve normally (Rodriguez-Alonso *et al.,* 2020). Early embryo loss in dairy cows can be as high as 25~41% on days 8~27 after insemination, leading to increasingly low reproduction rates and limiting the growth of the dairy industry (Yang *et al.,* 2024).

Embryo implantation occurs within a specific window (Dimova *et al.,* 2025). Successful implantation depends on the quality of the blastocyst, the exchange of information between the mother and fetus, and receptivity of the endometrium to the embryo. The success rate of implantation in animal embryo transfers is generally accepted to be approximately 25%, whereas 75% of implantation failures are owing to inadequate endometrial tolerance, contributing factors include chronic endometritis, mechanical injury secondary to dystocia, suboptimal endometrial perfusion, and exposure to endocrine-disrupting chemicals. (Rodríguez-Eguren *et al.,* 2024). Therefore, considerable endometrial tolerance is a prerequisite for effective information exchange between the mother and fetus, and for successful implantation, provided that the embryo is of reasonable quality.

Endometrial luminal epithelial cells (ELECs) are the first point of contact for blastocyst implantation. In the non-reproductive state, ELECs maintain a high degree of apical–basal and planar polarities, making them

unsuitable for fusion and invasion between the endometrium and polarized trophoblasts (Shibata *et al.,* 2024). During peri-implantation, the endometrial epithelium undergoes functional changes in morphology and structure in response to the coordinated action of steroid hormones, local endometrial molecules, and embryonic factors, a process known as plasma membrane transformation (PMT) (Akaeda *et al.,* 2024; Murphy and Shaw, 1994). This process is characterized by a transient loss of epithelial cell polarity, cytoskeletal remodeling, cell rearrangement, increased cell migration and motility, and acquisition of stromal cell characteristics for accommodating trophoblast invasion (Akaeda *et al.,* 2024) (Whitby *et al.,* 2020a). During this period, ELECs transmit embryonic signals to other tissues in the uterine lumen to synergistically establish endometrial tolerance for blastocyst implantation (Shang *et al.,* 2025). Abnormalities in PMT directly reduce endometrial tolerance and the success of embryo implantation (Jin *et al.,* 2025) (Whitby *et al.,* 2020a).

Existing studies on endometrial PMT have primarily focused on tissue cell morphology; however, the molecular mechanisms regulating PMT and its relationship with the establishment of endometrial tolerance remain poorly understood. Embryo implantation and tumor invasion are restricted by space and time, and share similar phenotypes and mechanisms (Borday *et al.,* 2018). Therefore, we hypothesize that shared molecular regulatory mechanisms may exist between these two. The Wnt signaling pathway is considered a crucial factor, which influences endometrial development and function (Wang *et al.,* 2024). It is associated with structural and functional changes in the endometrium before and during implantation and is influenced by hormonal regulation during the menstrual cycle and pregnancy.

Interferon-tau (IFN-τ), a pregnancy recognition signal specifically secreted by ruminant embryonic trophoblast cells, performs biological functions similar to those of progesterone and human chorionic gonadotropin (hCG), and regulates endometrial tolerance (Wiltbank *et al.,* 2023). Scattering proteins dishevelled (DVL/Dsh), including dishevelled segment polarity protein DVL1, DVL2, and DVL3 are central components of the Wnt/JNK signaling pathway, receiving upstream Wnt signaling in the cytoplasm and stabilizing free β-catenin by inhibiting the degradation complex (Maurice and Angers, 2025). Accordingly, we hypothesized that IFN-τ, as an hCG-like embryonic signal, may mediate the Wnt signaling pathway for regulating PMT during the peri-implantation period of dairy cows owing to the particularity of its secretion period. This study aimed to elucidate the molecular mechanism of PMT in ELECs regulated by IFN-τ, clarify its relationship with endometrial tolerance, and provide a basis for establishing clinical techniques to identify and intervene in endometrial tolerance.

MATERIALS AND METHODS

Isolation and transfection of primary bovine endometrial luminal epithelial cells (bELECs): Healthy Holstein cows (n=9) synchronized for estrus and bovine endometrial tissues were obtained from a local dairy farm (Shiyan, China). Tissue samples were randomly harvested from either uterine horn within 1 hour of slaughter. All procedures were approved by the Animal Ethics Committees of Huazhong Agricultural University (HZAUMO-2015-12) and Gansu Agricultural University (GSAU-Eth-VMC-2025-045). Primary bELECs were isolated using pronase E (Sigma, USA) digestion and mechanical scraping (Zhang *et al.,* 2021). Briefly, uterine tissues were rinsed with DPBS containing 50 IU/mL penicillin, 100 μg/mL streptomycin, and 2.5 μg/mL amphotericin B (Gibco, USA) for 2 h. The endometrium was digested with 1% streptomycin to obtain a cell suspension. Cells were cultured in DMEM/F-12 with 15% FBS (FBS, HYcezmbio, Wuhan, China) at 37 °C under 5% CO_2. Cell purity was assessed by CK-18 immunostaining. At 50%~70% confluence, cells were transiently transfected with DVL3 overexpression plasmid (pEX1-DVL3, GenePharma, China), siRNA or SuperTopFlash /SuperFopFlash reporters (D2505, D2507, Beytime, Shanghai, China) using Lipofectamine 3000. The transcriptional activity of the Wnt/β-catenin signaling pathway in bELECs was quantitatively assessed using the SuperTopFlash/SuperFopFlash reporter system. All primers and plasmids in Supplementary Table S1.

RNA isolation and qPCR: Total RNA was extracted using TRIzol (Invitrogen, USA), reverse-transcribed with HiScript III or miRNA cDNA Synthesis Kit (Vazyme, Nanjing, China), and analyzed by qPCR. Gene expression was normalized to *GAPDH* (mRNA) or *U6* (miRNA). Primers are listed in Supplementary Table S1.

Protein extraction and western blot: Proteins were extracted using RIPA buffer (Beyotime, China). Membrane, plasma, and nuclear proteins were isolated using commercial kits (Beyotime, China). Protein concentration was determined using BCA assay (Thermo Fisher Scientific, MA, USA). Immunoblotting followed standard protocols (Ma *et al.,* 2021) with antibodies listed in Supplementary Table S2.

Histopathology and immunostaining: H&E staining was used to assess histopathology. For immunohistochemistry (IHC), sections were subjected to antigen retrieval, peroxidase inactivation (3% H_2O_2), primary antibody incubation, and DAB (1:100, DAKO, K3468) visualization. For immunofluorescence (IF), permeabilized samples were blocked in 1% BSA, incubated with primary/secondary antibodies, and nuclei counterstained with DAPI. Images were captured via confocal microscopy. Antibodies are detailed in Supplementary Table S2.

Transmission and Scanning Electron Microscopy (TEM/SEM): Samples were fixed in 2.5% glutaraldehyde and postfixed with 1% osmium tetroxide. For TEM, specimens were dehydrated through graded ethanol, critical-point dried, sputter-coated, and imaged. For SEM, after ethanol/acetone dehydration, permeabilization was conducted under varying conditions (35°C/12 h, 45°C/12 h, or 60°C/24 h), followed by uranyl acetate and lead citrate staining prior to imaging.

Table S1: All Primers

Name	Primers (5'-3')
pEX1-DVL3	atgggcgagaccaagatcatctaccacctggacgggcaggagacgccgtacctggtgaagctgcccctgcccgccgagcgcgtcaccttggcggactttaagggcgttctgcaacgacccagctat aagttcttcttcaagtctatggacgacgatttcggagtggtgaaggaggagatctcggacgacaatgccaagctgccctgcttcaatggccgggtggtgtcctggctggtgtcggctgaaggctcacac ccagaaccagcagccttctgtgctgacagcccggcagaactgccaccgcccatggagcgcacaggaggcattggcgactcccggcccccatccttccaccctcacgctggtgggggcagccagga gaacctggacaatgacacagagactgactccttggtgtctgcccagcgagagcggccacgccggagggatggcccagagcacacaacccggctgaatggaactgccaaggggagcggcgacgag agccaggggttatgacagctcctccacccctgatgagcagcgagttggagaccaccagcttctttgattcagatgaggatgattccaccagcagcctggtggggaacgactgtgggcccacaggttc agcagctccacagagcagagcagcgcctcacgcctgatgagaagacacaagcggcggcggcggaagcagaaggtttcccggattgagcggtcttcatccttcagcagcatcacggactccaccatg tcactcaacatcatcaccgtcactctcaacatggaaaagtataacttcttgggcatctccatcgtgggccaaagcaacgagcgtggtgatggaggcatctacatcggctccatcatgaagggtggggc cgtggctgctgatggacgcattgagccaggagacatgctgttacaggtaaacgagatcaactttgagaacatgagtaacgatgacgcagtccgagtacttcgggaaattgtgcacaaaccagggccca tcaccttgactgtagccaagtgctgggacccaagtccacgtgggtgcttcacactgcccaggagtgagcccatccggcccattgaccccgcggcctgggtctcccacactgcagccatgaccggca ccttccctgcctacggcatgagcccttccctgagcaccatcacctccaccagctcctccatcaccagctccatccctgacacagagcgcctagacgacttccacctgtccatccacagtgacatggc tgccatagtaaaagccatggcctcccctgaatccgggctagaggtccgtgaccgaatgtggctcaagattaccattcccaacgctttcatcggctcggatgtggtggactggctgtaccacaacgtgg aaggcttcactgaccggcgagaggcccgcaagtatgccagcaacctgctgaaagctggcttcatccgccacactgtcaacaagatcaccttctccgagcagtgctactacatcttcggcgacctctg tggcaacatggccaacctctccctccacgatcacgacggctccagcggcgcctccgaccaggacacgctggcccctctgccgcacccaggggccgctccttggcccatggctttcccttaccagta cccgccgcccccacacccctacaatccgcacccaggcttcccagagctggggtacagctatggcgggggcagcgccagtagtcagcacagtgaaggcagccggagcagtgggtccaatcgtagcg gcagcgaccggcggaaggagaaggaccctaaggccggggactcgaagtcgggcggcagtggcagcgaatcggaccacacgacccgcagcagtctgcgggggccgcgggagcgggcgcccagcg agcgctcgggtcctgccgccagcgagcatagccaccgcagccaccactcgctggccagcagcctgcgcagccatcacacgcacccaagctacggccccctggggtgcccccctctctacgggcc ccccatgttgatgatgcccccaccgcccgcggccatggggccccgggagcccctccgggccgcgacctggcctctgtgcccccgaactgaccgccagcagacagtccttccgcatggccatgg gaaaccccaccaagaatttcgggctgtttgactttctgtga
Si-DVL3	F : GCGUCACCUUGGCGGACUUTT
	R : AAGUCCGCCAAGGUGACGCTT
Si-NC	F : UUAAGUGAUGCAAUAAUGUTT
	R : GCAUUAUUGCAUCACUUCATT
bta-GAPDH	F : GGCAAAGTGGACATCGTCGC
	R : GTTCACGCCCATCACAAACA
bta-DVL3	F : TACTACATCTTCGGCGACCT
	R : ATTGTAGGGGTGTGGGGG
bta-RAC2	F : GCCTATCACCTACCCGCA
	R : TCAAAACCATCTGGCTGGGAAG
bta-LIF	F : TCTGTCTTACAACACAGGCTCC
	R : CACTGCTGTTGAGTTGTCCC
bta-ITGB3	F : TTCAGCATTGAGGCCAAAGT
	R : AAGGTCCCATTGCCATTGTT
bta-HOXA10	F : AAGGTCCCATTGCCATTGTT
	R : CTTCAGTTTCATCCTGCGGT
bta-ISG15	F : GTCTTTTGAAGGGAGGCCCA
	R : CTACCCACCCCGAAGACGTA
bta-ISG12	F : TGCAGAACTGCATCTCCATC
	R : TTCATGAGGCCGTATTCCTC
bta-MX1	F : GAAGAGCCTGCTGTGGACAT
	R : TTTGGACTTGGCAGTTCGGT
bta-MX2	F : GGTCCACCTGAACGCATATT
	R : TCATGGCTTTCTGGACCTTATC
bta-TCF1	F : ACAACTGGTTTGCCAATCGC
	R : TGCTCAGCAGACTGTGACTG
bta-MMP7	F : TTGCAACACATGAGCTTGGC
	R : GAAGACGGGAACAGTGCTCA
bta-MUC1	F: CTGGTCCTGGTCTGTGTTCT
	R: CTTACAAGTTGGCGGAAGTG
bta-ESR1	F: ACGATTGATAAAAACAGGAGGAAG
	R: GCCTTTCATCATGCCCACTT

Table S2: Information on antibodies used in the study

Antibodies	Catalogs	Dilution	Species	Manufacturer
β-actin	#4970	1:1000 (WB)	Rabbit	Cell Signaling Technology
GAPDH	GB12002	1:1000 (WB)	Mouse	Servicebio
Anti-rabbit IgG	#5127	1:2000 (WB)	Mouse	Cell Signaling Technology
Anti-mouse IgG	#7056	1:2000 (WB)	Goat	Cell Signaling Technology
CK18	GB11232	1:200 (IF)	Rabbit	Servicebio
Cy3 anti-rabbit IgG	GB21303	1:100 (IF)	Goat	Servicebio
Cy3 anti-mouse IgG	GB21301	1:100 (IF)	Goat	Servicebio
FITC anti-mouse IgG	GB22301	1:50 (IF)	Goat	Servicebio
FITC anti-rabbit IgG	GB22303	1:50 (IF)	Goat	Servicebio
Phalloidin-iFluor^{TM}488 Conjugate	#23115	1:1000 (IF)	-	AAT Bioquest
DVL3	#3218	1:1000 (WB), 1:100 (IP)	Rabbit	Cell Signaling Technology
DVL3	A3842	1:1000 (WB), 1:50 (IF), 1:100 (IHC)	Rabbit	ABclonal
RAC2	A1139	1:2000 (WB), 1:100 (IF), 1:100 (IHC)	Rabbit	ABclonal
MUC1	Ab233933	1:1000 (IHC)	Mouse	abcam
β-catenin	ab16051	1：1000 (WB), 1:500 (IHC)	Rabbit	abcam
E-cadherin	sc-8426	1:1000 (WB), 1:200 (IF)	Mouse	Santa Cruz Biotechnology
N-cadherin	#13116	1:1000 (WB), 1:200 (IF), 1:125 (IHC)	Rabbit	Cell Signaling Technology
HOXA10	LS-B10575/56389	1:2500 (WB), 1:100 (IHC)	Goat	LifeSpan BioSciences

Real-time cell adhesion assay (RTCA): Cell adhesion was dynamically monitored using xCELLigence RTCA DP. Briefly, 3×10^4 cells were seeded in a CIM-Plate 16, and 100 µL fresh medium was added each well. After system self-testing and baseline verification (Cell Index <0.063), impedance was recorded every 15 min. Data were evaluated using the RTCA-DP software (Roche Diagnostics GmbH, Mannheim, Germany).

Cell viability assay: Cell viability was determined using Cell Counting Kit-8 (CCK8, MCE, HY-K0301). 2×10^4 cells/ in 96-well plates were treated with CCK-8 reagent for 1~3 h. Absorbance at 450 nm was measured using a microplate reader (Bio-Rad, USA).

Transwell migration and invasion assays: For migration assay, transfected bELECs in serum-free medium were seeded into Transwell inserts (8µm, Corning, USA)), with 10% FBS medium as a chemoattractant in the lower chamber. After 4~6 h, migrated cells were fixed, stained with crystal violet, and quantified. Invasion assays were performed similarly using Matrigel (BD Biosciences, USA) -coated chambers (300 µL, 37 °C, 1 h).

Wound healing assay: Confluent bELECs were serum-starved for 24 h, and a linear scratch was made using a pipette tip. Wound closure was monitored over 30 h in complete medium and analyzed microscopically (Olympus, Japan).

Co-immunoprecipitation: Cell lysates from bELECs were immunoprecipitated overnight with anti-DVL3 antibody at 4°C, followed by protein A/G bead pulldown (36403ES08, Yesheng, Shanghai, China). Precipitated complexes were analyzed via Western blot to detect RAC2 interaction.

Statistical analysis: Data from more than independent experiments are expressed as mean ± standard error. Statistical significance was analyzed using an unpaired Student's t-test or one/two-way ANOVA with Sidak's multiple comparison test. ANOVA was used to compare more than two groups. Statistical significance was set at $P<0.05$.

RESULTS

Bovine endometrium undergoes plasma membrane transformation during the peri-implantation period: Analysis of bovine endometrial RNA sequencing data (GSE171577, $P<0.05$ and $\log_2|FC|>2$) (Martins *et al.,* 2022b) revealed the top 60 DEGs were enriched in actin cytoskeleton, adhesion spots, mucins, and extracellular matrix receptor interactions pathways (Fig S1). This implies that the endometrium may undergo plasma membrane transformation during implantation in dairy cows.

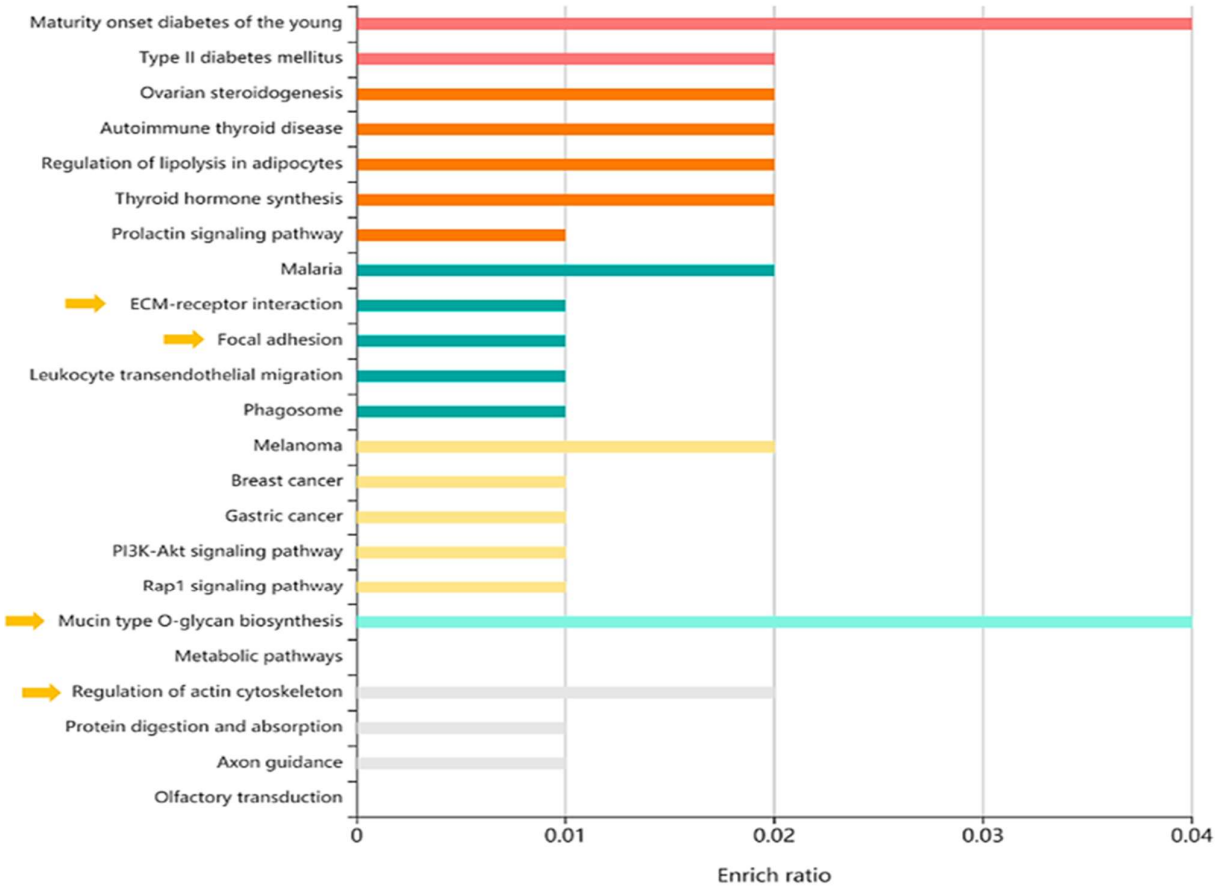

Fig. S1: Identification of DEGs in the pregnant bovine endometrium from the GEO dataset (GSE107891) and supplement data from a previous study(Martins *et al.,* 2022a). $P<0.05$, $|\log FC| > 2$. The top 60 GO (biological process) term of differentially expressed genes in the endometrium on day 4 of estrus and day 30 of pregnancy after progesterone treatment.

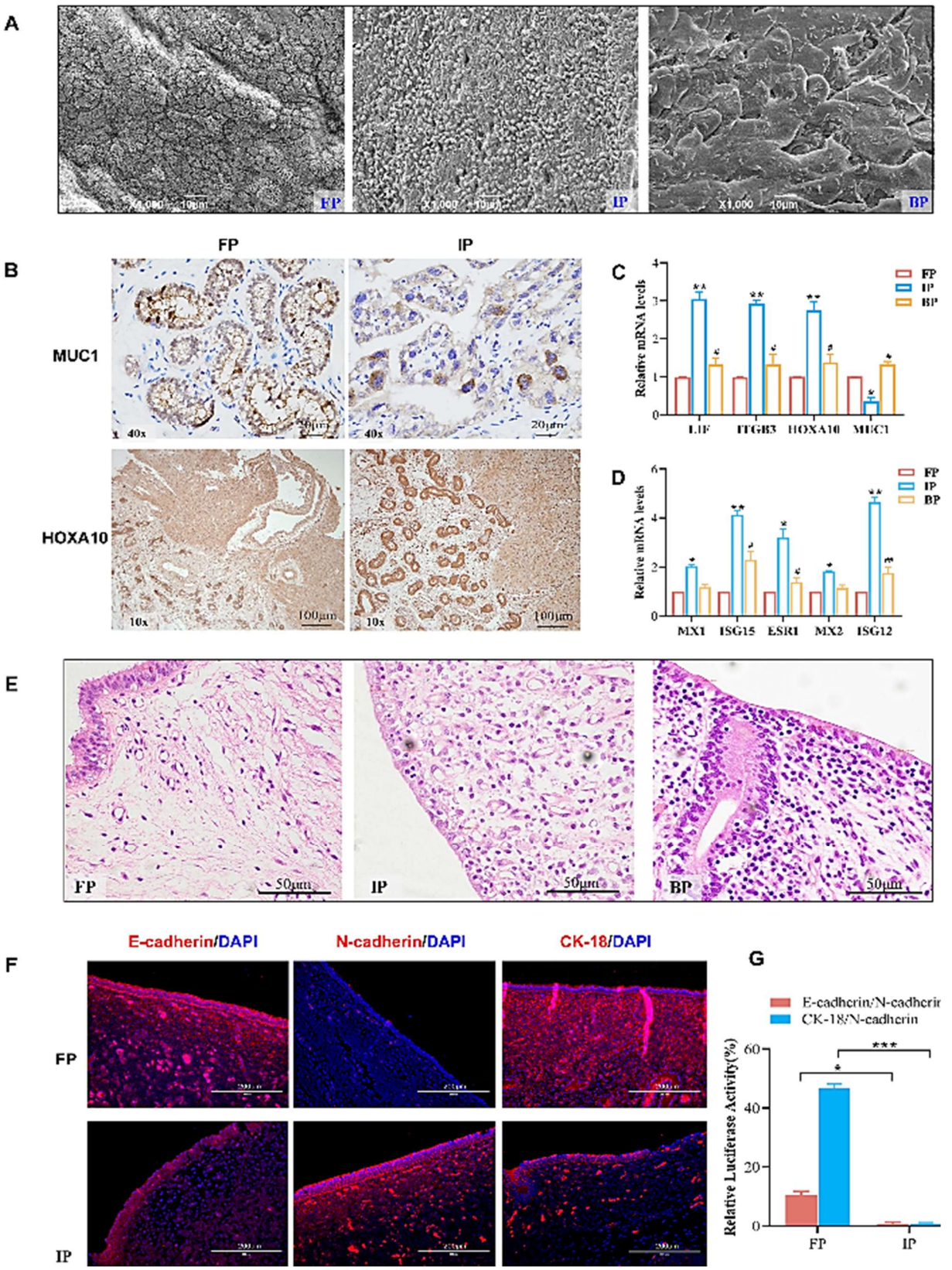

Fig. 1: Bovine endometrium undergoes plasma membrane transformation during the peri-implantation period. (A) SEM images of the bovine endometrium in the peri-implantation period. Scale bar, 10 μm. (B) Endometrial receptivity markers HOXA10 (10×) and MUC1 (40×) by IHC. (C) mRNA levels of *LIF, ITGB3, HOXA10*, and *MUC1*. (D) mRNA levels of IFN-τ-stimulated genes *MX1, ISG15, ESR1, MX2,* and *ISG12*. (E) Endometrial morphology. Scale bar, 50 μm. (F-G) Immunofluorescence and semiquantitative analysis of PMT markers (E-cadherin, N-cadherin, CK18; scale: 200 μm). Data are presented as mean ± SEM (n=3). FP:peri-implantation; IP:peri-implantation; BP:post-implantation.*P<0.05 indicates a significant difference between peri-implantation and peri-implantation; #P<0.05 indicates a significant difference between post-implantation and peri-implantation. *P<0.05, **P<0.01, ***P<0.001, #P<0.05, ##P<0.01.

To assess plasma membrane transformation, bovine endometrial tissues from three gestational periods (peri-implantation, FP; implantation, IP; post-implantation, BP) were examined by SEM. Dense microvilli predominated peri-implantation, mature pinopodes emerged during implantation, and pinopodes became rare with irregular microvilli post-implantation (Fig. 1A). IHC showed that homeobox A10 (HOXA10) was enriched in the endometrial glands during implantation, whereas mucin 1 (MUC1) expression was significantly reduced at implantation compared to the peri-implantation period (Fig. 1B). Consistently, qPCR confirmed that the transcript levels of leukemia inhibitory factor (*LIF), integrin subunit beta 3 (ITGB3)*, and *HOXA10* were higher, and that of *MUC1* was lower in the implantation period (Fig. 1C). Meanwhile, the mRNA levels of MX dynamin like GTPase 1 (*MX1),* interferon stimulated gene 15 (*ISG15)*, and estrogen receptor 1 (*ESR1)* were upregulated during implantation (Fig. 1D), indicating that they were regulated by IFN-τ (a pregnancy recognition signal secreted by peri-implantation embryonic trophoblasts in ruminants). These findings demonstrate that morphological and molecular changes in endometrial epithelium during implantation create a receptive condition for embryonic trophoblast adhesion and fusion, validating the timing of endometrial tissues collection.

Morphology showed enriched microvilli and a clearly arranged monolayer of nuclei with obvious apical–basal cell polarity in bELECs during implantation. Conversely, endometrial surfaces were smooth with irregular nuclei arrangement and lost polarity during peri-implantation and post-implantation periods (Fig. 1E). Phalloidin staining revealed an increased polymerization and rearrangement. Epithelial cadherin (E-cadherin) and CK18 were markedly under expressed in bELECs during implantation, whereas N-cadherin were strongly expressed (Fig. 1F, G). Collectively, these findings suggest endometrial epithelial cells undergo plasma membrane transformation during implantation, establishing structural basis for endometrial receptivity in dairy cows.

Interferon-tau facilitates the establishment of endometrial receptivity in dairy cows: Interferon-tau acts on bELECs in a paracrine manner. To investigate its role in bovine endometrial receptivity, primary bELECs were isolated and cultured. First-generation cells (95% purity assessed using CK18, Fig. 2A and Fig S2A) were treated with IFN-τ (0, 100, or 200 ng/mL) for 12 h. IFN-τ at 200 ng/mL barely affected cell viability (Fig. 2B) but significantly upregulated *MX1, ISG15*, and *ESR1* transcript levels, indicating a successful *in vitro* IFN-τ model (Fig. 2C). Subsequent qPCR demonstrated that 200 ng/mL IFN-τ induced significant expression of receptivity *HOXA10* and *ITGB3* in bELECs and bovine endometrial epithelial cell line (BEND) (Fig. 2D), confirming IFN-τ enhancing endometrial receptivity.

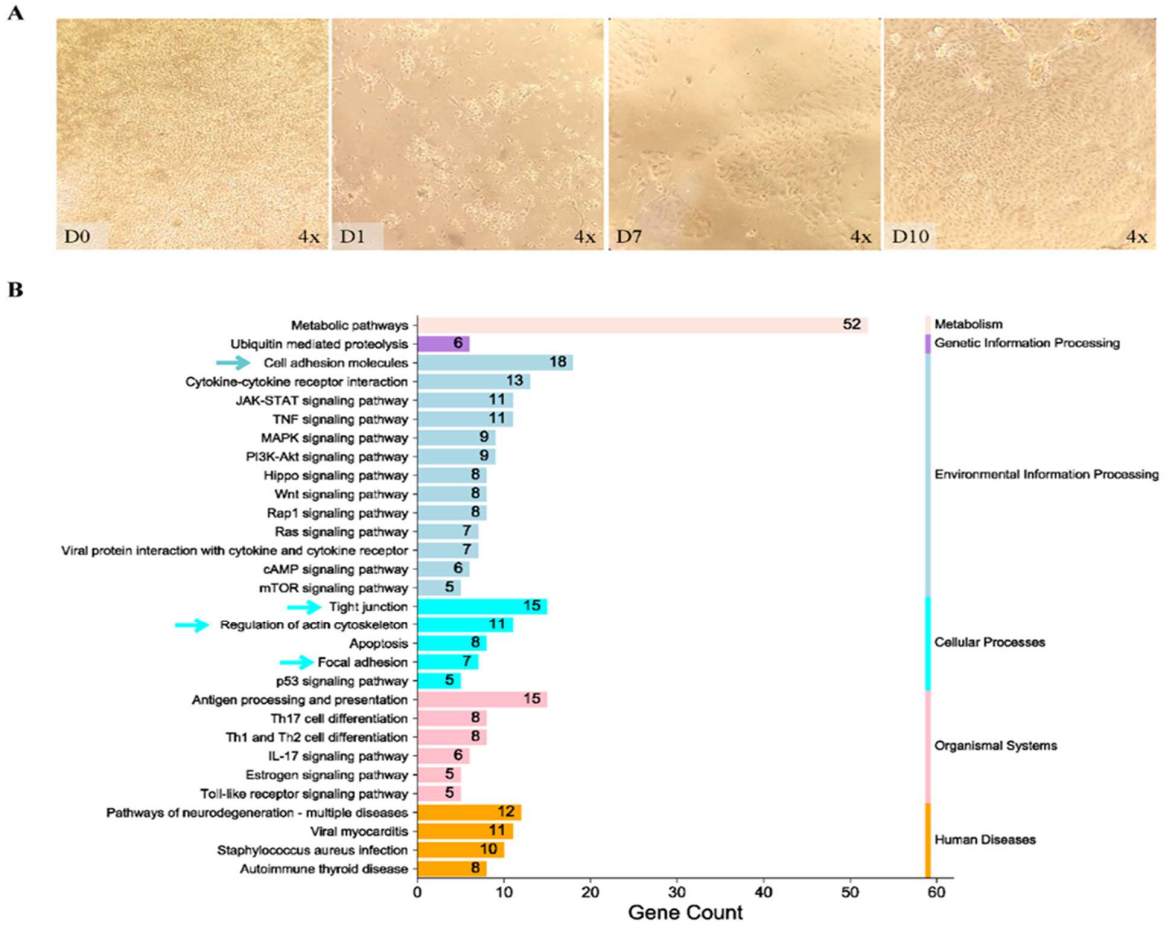

Fig. S2: (A) Morphological characterization of primary bELECs (passage 1) under bright-field microscopy at consistent magnification. Images were captured at D0 (immediately after seeding), D1, D7, and D10 of the primary culture. (B) KEGG analysis of IFN-τ-induced DEGs in bELECs. Blue arrows highlight pathways linked to plasma membrane transformation.

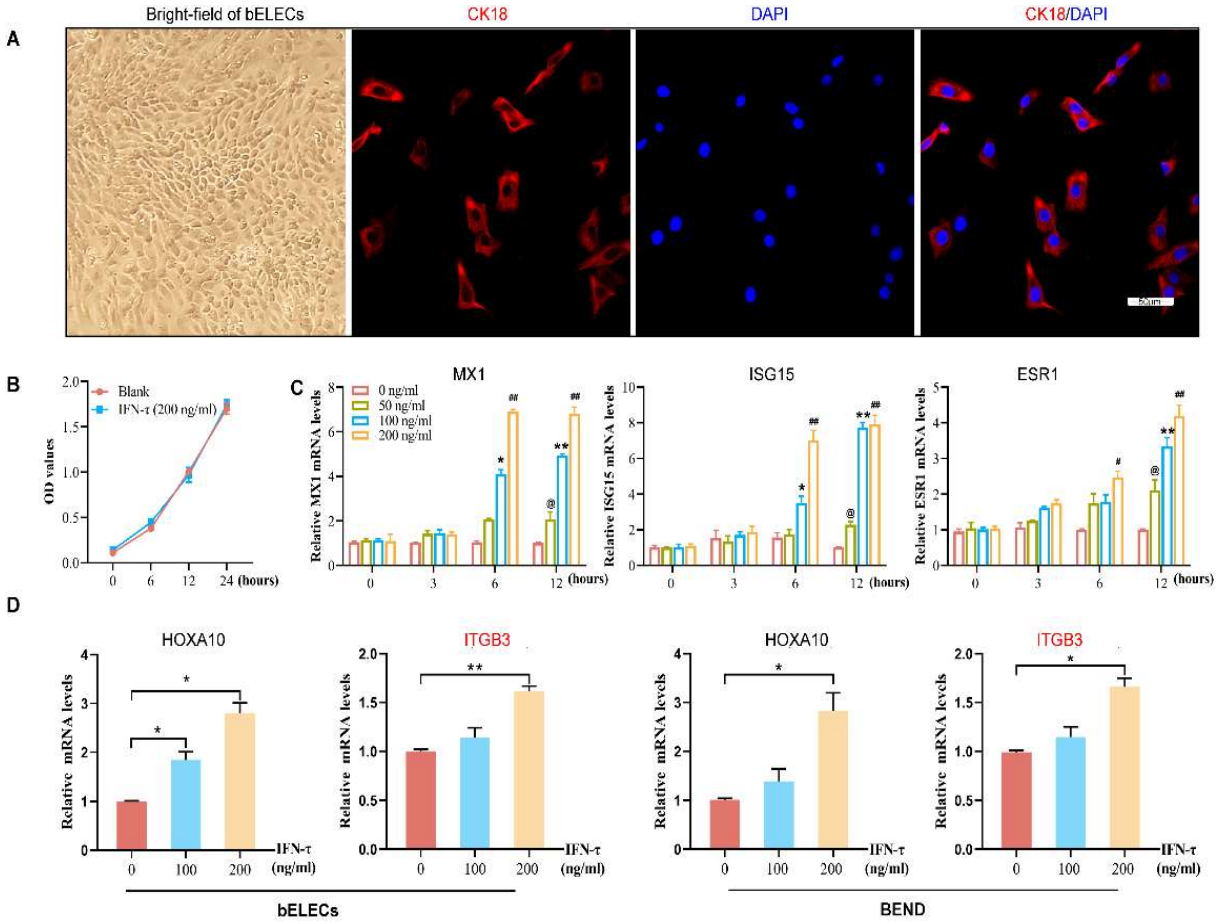

Fig. 2: Interferon-tau facilitates the establishment of endometrial receptivity in dairy cows. (A) Morphological characteristics of bovine endometrial luminal epithelial cells under bright-field microscopy and identification by CK18 immunofluorescence following subculture. (B) Effect of IFN-τ (200 ng/mL) on bELEC proliferation. (C) mRNA levels of IFN-τ-stimulated genes *MX1, ISG15*, and *ESR1* in bELECs. (D) mRNA levels of *HOXA10* and *ITGB3* in bELECs and BEND. Data are presented as mean ± standard of three independent experiments (n=3). Statistical significance compared to the blank group (0 ng/mL) is indicated as follows, $^{@}$P<0.05 for the 50 ng/mL group; *P<0.05 for the 100 ng/mL group; $^{\#}$P<0.05 for the 200 ng/mL group.

Interferon-tau induces plasma membrane transformation in bovine endometrial luminal epithelial cells: Interferon-tau induces 707 differentially expressed genes (DEGs) enriched in tight junctions, cytoskeletal regulation and adhesion spots (Zhao *et al.,* 2018) (Fig S2B). Integrated analysis with previous GSE171577 data suggests IFN-τ is inferred to regulate cytoskeleton and cell adhesion, driving plasma membrane transformation in bELECs. Thus, its impact on plasma membrane transformation markers were examined. Fulvestrant (100 nM) and mifepristone (30 μM) were used to negate estrogen and progesterone on primary bELECs, showing minimal impact on PMT markers (Fig. 3A, B). Subsequent experiments used fourth-generation bELECs. SEM revealed IFN-τ disrupted intercellular typical tight junction, degenerated microvilli, and expanded intercellular spaces (Fig. 3C). IF indicated IFN-τ significantly downregulated the expression of E-cadherin and CK18 while upregulating N-cadherin and vimentin (Fig. 3A, B). RTCA-DP results demonstrated that upon IFN-τ treatment reduced transepithelial electrical resistance values (TEER, a marker of intercellular adhesion) (Whitby *et al.,* 2020b)(Fig. 3D), indicating weakened cellular adhesion among bELECs, which allows spatial conditions for embryo implantation. Collectively, IFN-τ induced plasma membrane transformation of bELECs.

Interferon-tau induces high expression of DVL3 and β-catenin in peri-implantation bovine endometrium: To delineate IFN-τ's role in PMT of bELECs, protein interaction network analysis of IFN-τ-induced DEGs identified DVL3 as a core regulator interacting with β-catenin (CTNNB1), E-cadherin (CDH1), and other adherens junction components (RAC2, RAC1, CTNND1, MUC1) (Fig. S3A). DVL3 mRNA and protein expression were significantly elevated in implantation-phase endometrium (Fig. 4A-B), with immunolocalization to bELEC cytoplasm and membranes (Fig. 4C). IFN-τ treatment directly induced DVL3 overexpression in bELECs (Fig. 4D-E). Although total β-catenin levels remained stable (Fig. 4F), nuclear accumulation increased significantly during implantation, activating transcription factors MMP7 and TCF1 (Fig. 4G). Functional validation through DVL3 overexpression (pEX1-DVL3) and knockdown (si-DVL3) experiments (Fig. S3B-D), combined with dual-luciferase reporter assays using SuperTopFlash and negative control SuperFopFlash plasmids in bELECs (Fig. 4H-I) and downstream signaling analysis (Fig. 4J), confirmed that IFN-τ enhances β-catenin transcriptional activity in a DVL3-dependent manner. These data demonstrate that IFN-τ drives plasma membrane transformation via DVL3-mediated activation of β-catenin nuclear translocation.

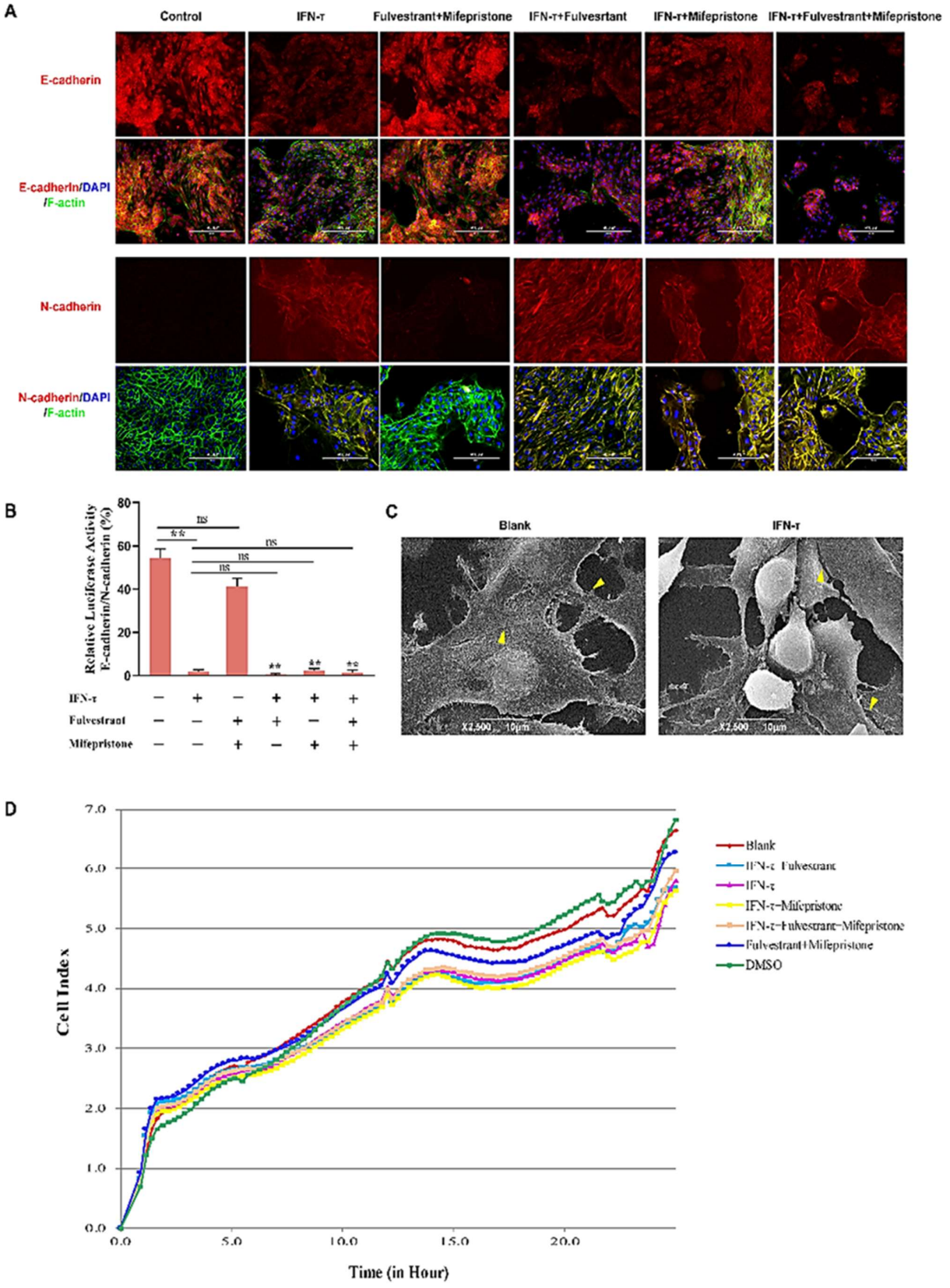

Fig. 3: Interferon-tau induces plasma membrane transformation in bovine endometrial luminal epithelial cells. (A, B) IF analysis of the localization and expression of E-cadherin and N-cadherin. (C) SEM characterization of PMT of bELECs (2500×). Scale bar, 10 μm. The yellow arrows indicate connections between bELECs. Blank, the control group without IFN-τ intervention; IFN-τ, IFN-τ (100 ng/mL) treatment group. (D) Changes in the cross-cell impedance values of bELECs. Data are expressed as mean ± standard error of three independent experiments (n=3). $^{**}P<0.01$.

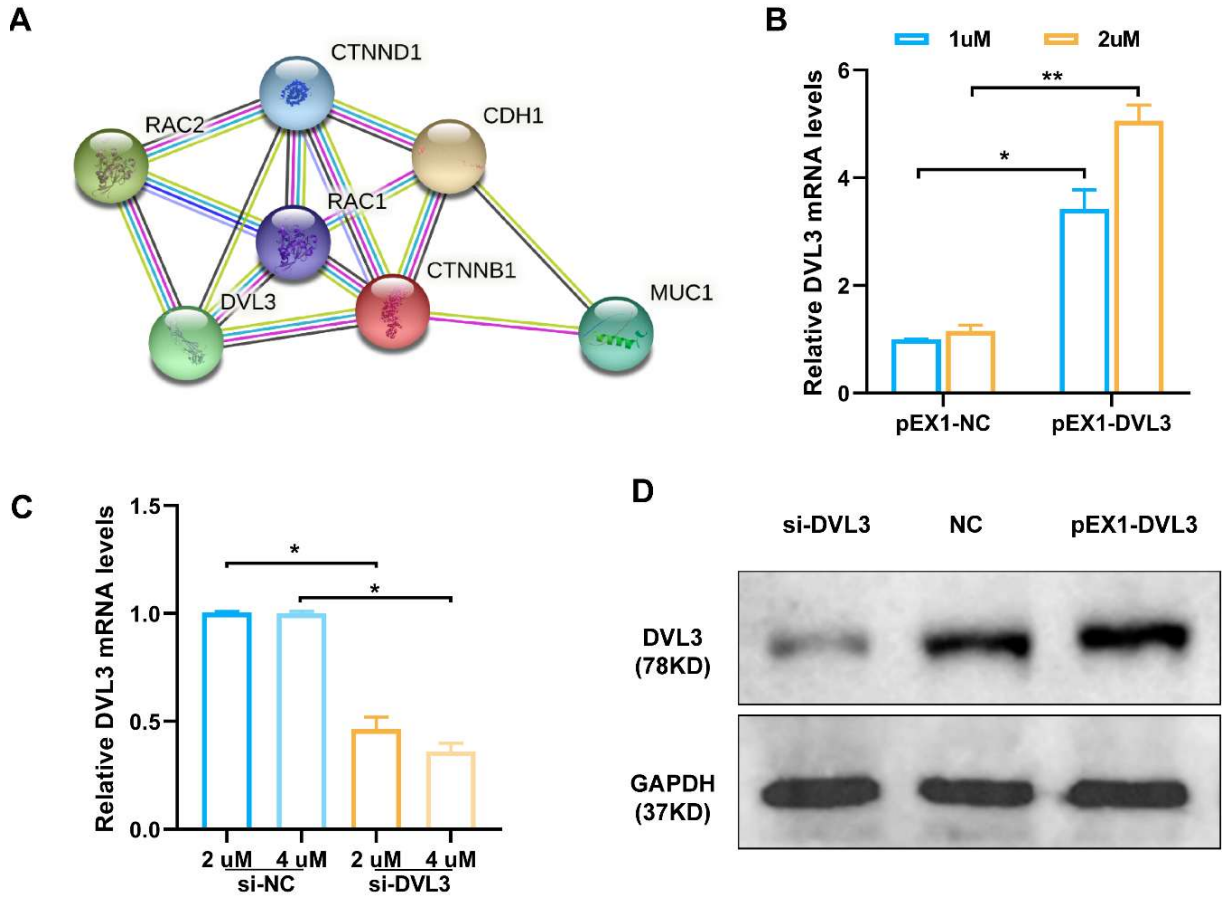

Fig. S3: (A) PPI network of core DEGs. (B) RT-qPCR confirmed pEX1-DVL3 efficiency, *P<0.05 vs. pEX1-NC. (C) si-DVL3 silencing efficiency and optimal concentration, *P<0.05 vs. si-NC. (D) WB detection of DVL3 protein expression after si-DVL3 and pEX1-DVL3 (n=3, GAPDH loading control). Values are given as the mean ± SEM.

DVL3 induces plasma membrane transformation of endometrial luminal epithelial cells by promoting cell migration and reducing cell adhesion: To elucidate the biological function of DVL3 in bovine endometrium during implantation, bELECs were transfected with pEX1-DVL3 and si-DVL3. IF showed that *DVL3* knockdown significantly increased E-cadherin/N-cadherin ratio in response to IFN-τ intervention (Fig. 5A, B), inhibiting PMT. Given parallels between PMT and epithelial-mesenchymal transition in cellular behavior (Murphy, 2004), we assessed DVL3's impact on bELEC migration and invasion. Silencing DVL3 markedly inhibited cell migration in scratch assays, while DVL3 overexpression enhanced motility (Fig. 5C, D), confirmed by Transwell migration assays (Fig. 5E). However, DVL3 did not affect IFN-τ-mediated invasion (Fig. 5F). RTCA-DP showed that bELECs exhibited a rapid proliferation trend and a gradual increase in transmembrane electrical resistance from 0 to 15 h. However, after 15 h, *DVL3* overexpression significantly decreased the TEER value (Fig. 5G), suggesting that DVL3 may lead to a decrease in intercellular adhesion by disrupting intercellular junctions.

DVL3 activates RAC2 to promote plasma membrane transformation in bovine endometrial luminal epithelial cells: Protein interaction analysis suggested a potential DVL3-RAC2 interaction, with AutoDock predicting a binding free energy of -16.31 kcal/mol and a dissociation constant of 1.09×10^{-12} M, demonstrating strong binding and high affinity that indicates RAC2 might interact with DVL3 to regulate PMT of bELECs. Elevated RAC2 mRNA and protein levels were observed in endometrial tissues of peri-implantation (Fig. 6A, B). IFN-τ upregulated RAC2 expression in bELECs, as shown by qPCR and IF (Fig. 6C, D). Laser confocal microscopy localized both DVL3 and RAC2 to the bELEC plasma membrane (Fig. 6E), and co-immunoprecipitation confirmed their direct interaction under IFN-τ (Fig. 6F). To explore their regulatory relationship, bELECs were transfected with pEX1-DVL3, si-DVL3, pEX1-RAC2, or RAC2 inhibitor EHT1864. WB revealed EHT1864 suppressed RAC2, an effect reversed by DVL3 overexpression (Fig. 6G), suggesting RAC2 as a downstream DVL3 effector. Functionally, RAC2 blockade with EHT1864 hindered PMT in bELECs, an inhibition reversed by DVL3 overexpression (Fig. 6H). SEM revealed DVL3-dependent enhancement of cellular adhesiveness through RAC2 activation (Fig. 6I). Furthermore, RAC2 blockade impaired endometrial receptivity, indicating its essential role in DVL3-mediated membrane remodeling and receptivity establishment (Fig. 6J). Therefore, RAC2 is crucial for maintaining normal plasma membrane transformation and receptivity establishment of bELECs.

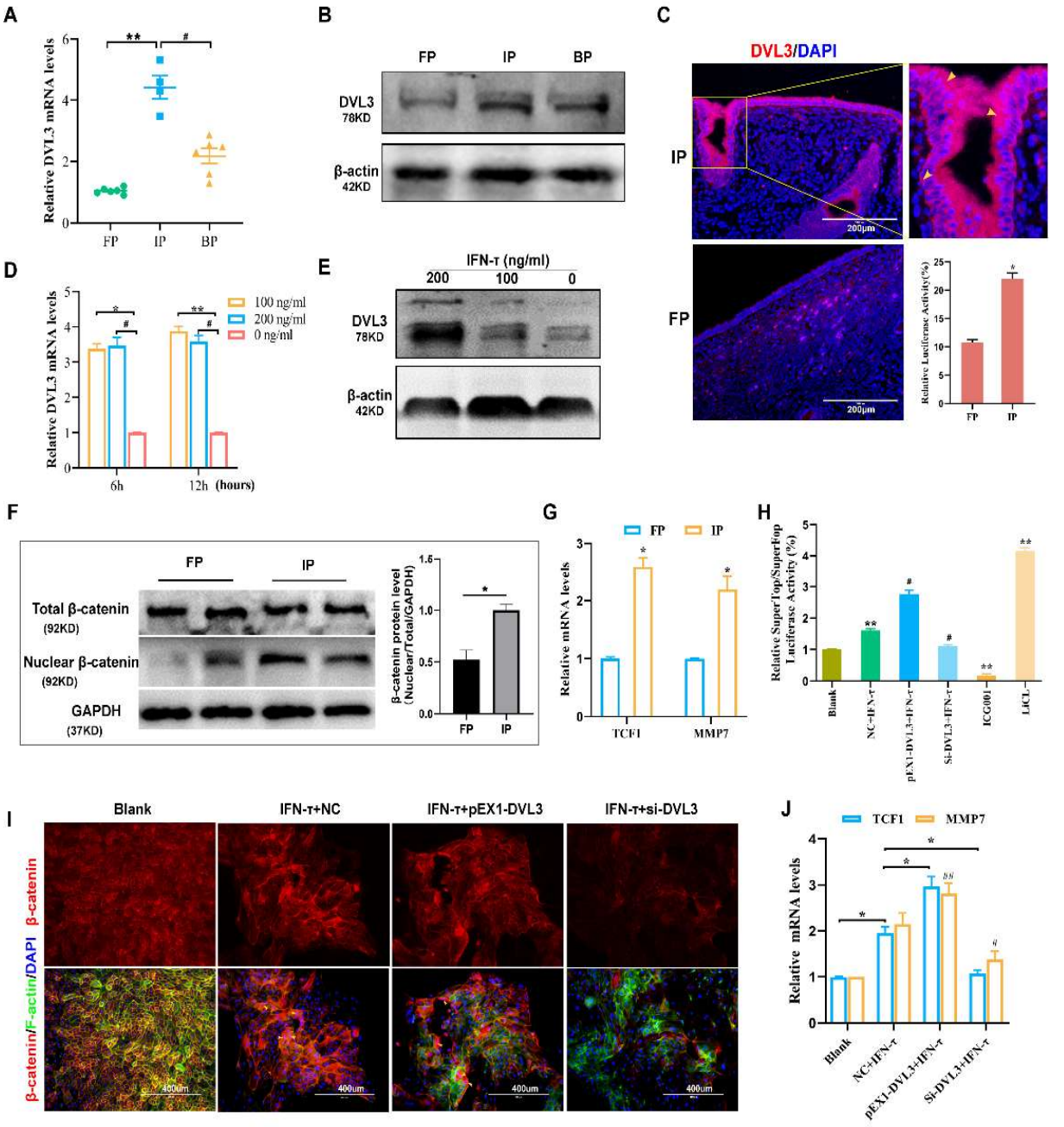

Fig. 4: Interferon-tau induces high expression of DVL3 and β-catenin in peri-implantation bovine endometrium. (A) mRNA levels of *DVL3* in bovine endometrial tissue. (B) DVL3 expression in bovine endometrial tissue (n = 3). The loading control was β-actin. (C) Expression and localization of DVL3 in bovine endometrial tissue. (D) mRNA level of *DVL3* under IFN-τ intervention. (E) DVL3 expression in bELECs treated with IFN-τ (n = 3). The loading control was β-actin. (F) Protein expression levels of nuclear β-catenin/total β-catenin in bovine endometrium, shown by WB (n = 3). The loading control was GAPDH. (G) mRNA levels of *TCF1* and *MMP7*. (H) SupTopFlash/SupFopFlash fluorescent reporter gene assay to detect the activation of β-catenin by DVL3 under IFN-τ intervention. LiCl (Wnt/β-catenin activator, positive control); ICG-001 (inhibitor, negative control). (I) Effects of overexpression and silencing of *DVL3* on β-catenin activation in bELECs. (J) mRNA levels of *TCF1* and *MMP7*. The results are presented as mean ± standard error of three independent experiments (n=3). *FP*:P*eri-imPlantation; IP*:P*eri-imPlantation; BP*:P*ost-imPlantation;* *P<0.05 and **P<0.01 indicate significant difference between the peri-implantation and blank groups without IFN-τ intervention. $^{\#}$P<0.05 and $^{\#\#}$P<0.01 vs. the IFN-τ intervention groups.

Polymerization of filamentous actin is regulated by DVL3/RAC2 signaling: Filamentous actin is a key member of actin dynamics. We observed that RAC2 and F-actin were positively expressed in the endometrium of peri-implantation dairy cows and were localized on the apical surface of bELECs (Fig. 7A). Blocking of RAC2 promoted F-actin depolymerization (Fig. 7B). In particular, treatment with EHT1864 directly blocked the induction of RAC2 by *DVL3* overexpression and prevented F-actin polymerization (Fig. 7B). Collectively, these findings suggest that F-actin polymerization is a downstream effector of RAC2 in maintaining plasma membrane transformation of bELECs.

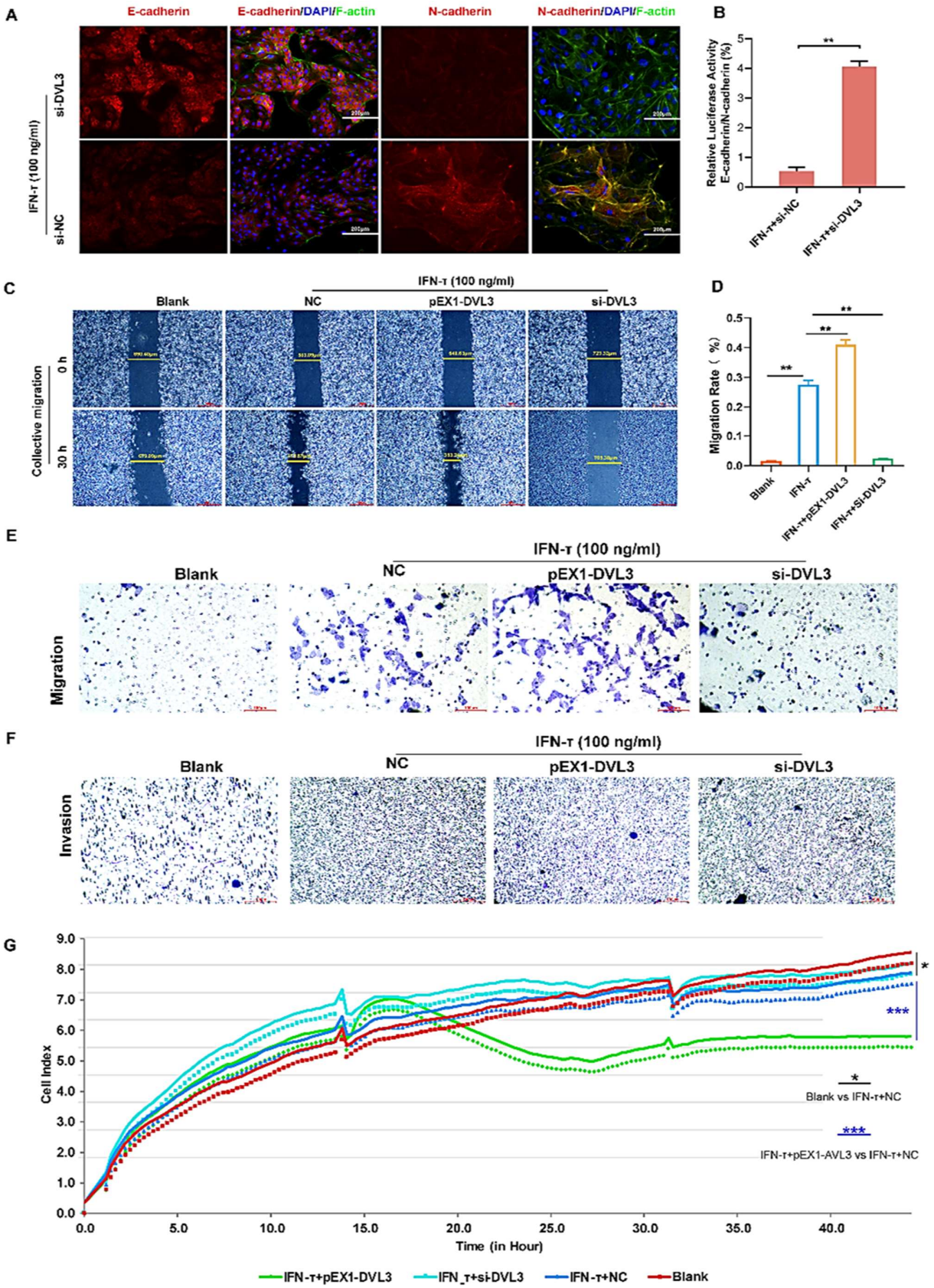

Fig. 5: DVL3 induces plasma membrane transformation of endometrial luminal epithelial cells by promoting cell migration and reducing cell adhesion. (A) Effect of *DVL3* silencing on plasma membrane transformation of bELECs. (B) Quantification of E-cadherin and N-cadherin expression. (C, D) Cell scratch assay to assess the effect of DVL3 on bELECs migration. Cell migration rates were measured using ImageJ software. (E) Transwell migration assay to measure bELEC migration. (F) Transwell invasion assay to detect bELEC invasion. (G) Changes in transcellular impedance values of bELECs with overexpressed or silenced *DVL3* in real time. The data are expressed as mean ± standard error of three independent experiments (n=3). $^{**}P<0.01$.

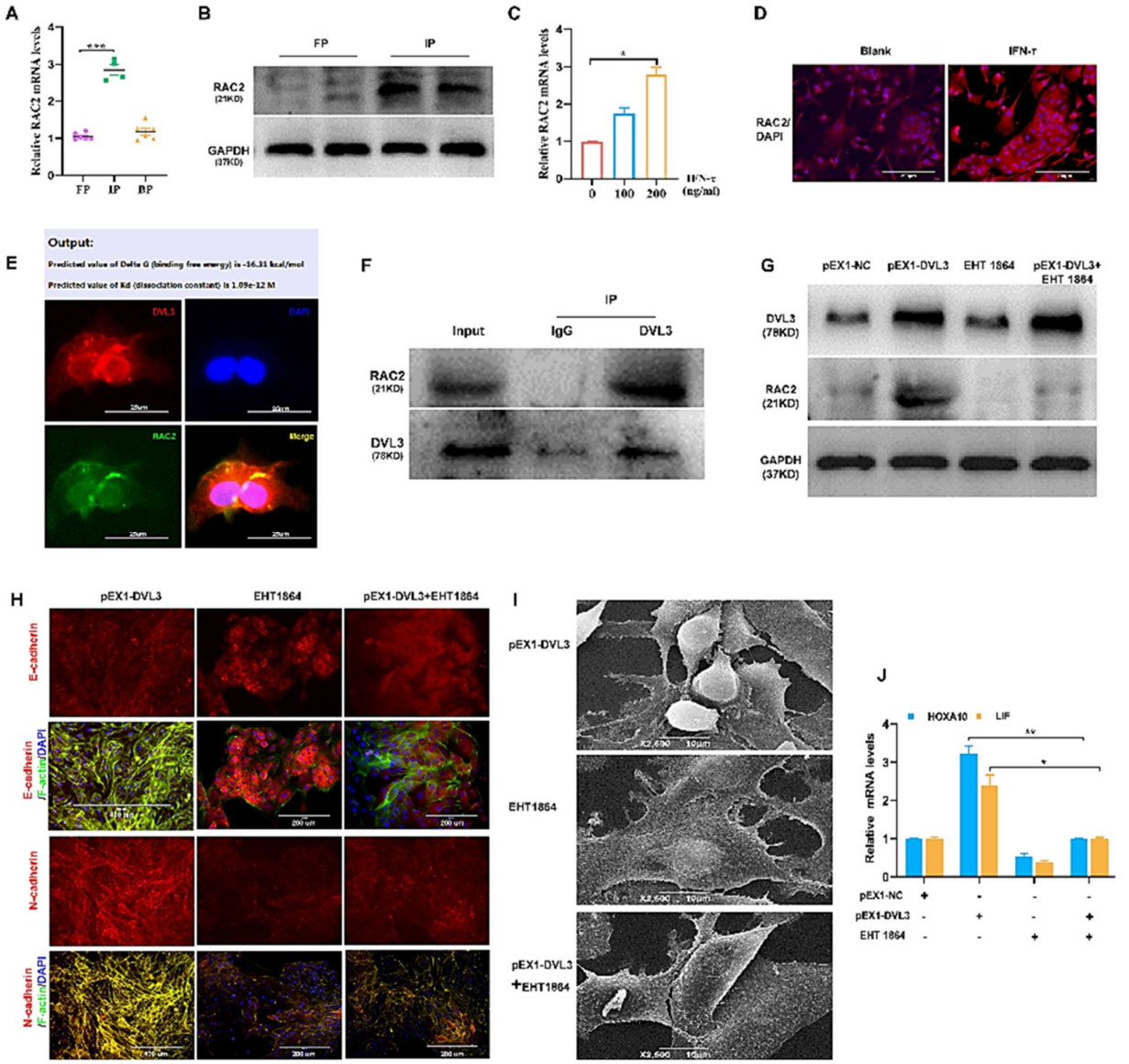

Fig. 6: DVL3 activates RAC2 to promote plasma membrane transformation in bovine endometrial luminal epithelial cells. (A) The mRNA expression levels of RAC2 in bovine endometrial tissue detected by RT-qPCR. (B) RAC2 expression in cow endometrial tissue (n = 3), *FP*:P*eri-im*P*lantation; IP*:P*eri-im*P*lantation*. (C) mRNA expression of *RAC2* under IFN-τ intervention. (D) RAC2 expression in bELECs under IFN-τ (100 ng/mL) intervention. (E) Laser confocal microscopic analysis of the subcellular localization of DVL3 and RAC2. (F) Analysis of interaction between DVL3 and RAC2. (G) DVL3 and RAC2 expression after *DVL3* overexpression and/or RAC2 inhibition (n = 3). (H) E-cadherin and N-cadherin expression after *DVL3* overexpression and/or RAC2 inhibition. (I) Scanning electron microscopic characterization of plasma membrane transformation of bELECs (2500×). Scale bar, 10 μm. (J) mRNA levels of *HOXA10* and *LIF* in bELECs after *DVL3* overexpression and/or RAC2 inhibition. GAPDH was used as a loading control. The data are presented as mean ± standard error of three independent experiments (n = 3). Comparisons between specific groups are indicated by the connecting lines, and *P<0.05 denotes significant difference.

DISCUSSION

Plasma membrane transformation is a conserved biological process critical for embryo implantation across species. Substantial evidence shows that endometrial epithelial cells undergo morphological and functional changes resembling epithelial-mesenchymal transition during implantation (Owusu-Akyaw *et al.,* 2019). This adaptation facilitates embryo attachment, as observed in humans (Oghbaei *et al.,* 2022), goats (Wango *et al.,* 1990), cat(Dudley *et al.,* 2018), and viviparous lizards (Murphy and Shaw, 1994). PMT enables membrane fusion between trophoblasts and endometrial epithelia (Whitby *et al.,* 2020a). Early in pregnancy, parallel membrane alignment occurs at the contact zone between trophoblasts and luminal epithelia(Oghbaei *et al.,* 2022). This dynamic interaction relies on basolateral membrane remodelling in endometrial cells. Though subtle and understudied in animals, our findings and prior reports consistently document this phenomenon in experimental models.

PMT manifests through structural changes, most notably in apical microvilli(Whitby *et al.,* 2020a). These dynamic projections define endometrial membrane plasticity and are a key focus of early-pregnancy ultrastructure studies. The uterus responds to ovarian steroid hormones. Progesterone alone induces short, uniform microvilli in human endometrial epithelia, whereas estrogen promotes long, slender microvilli

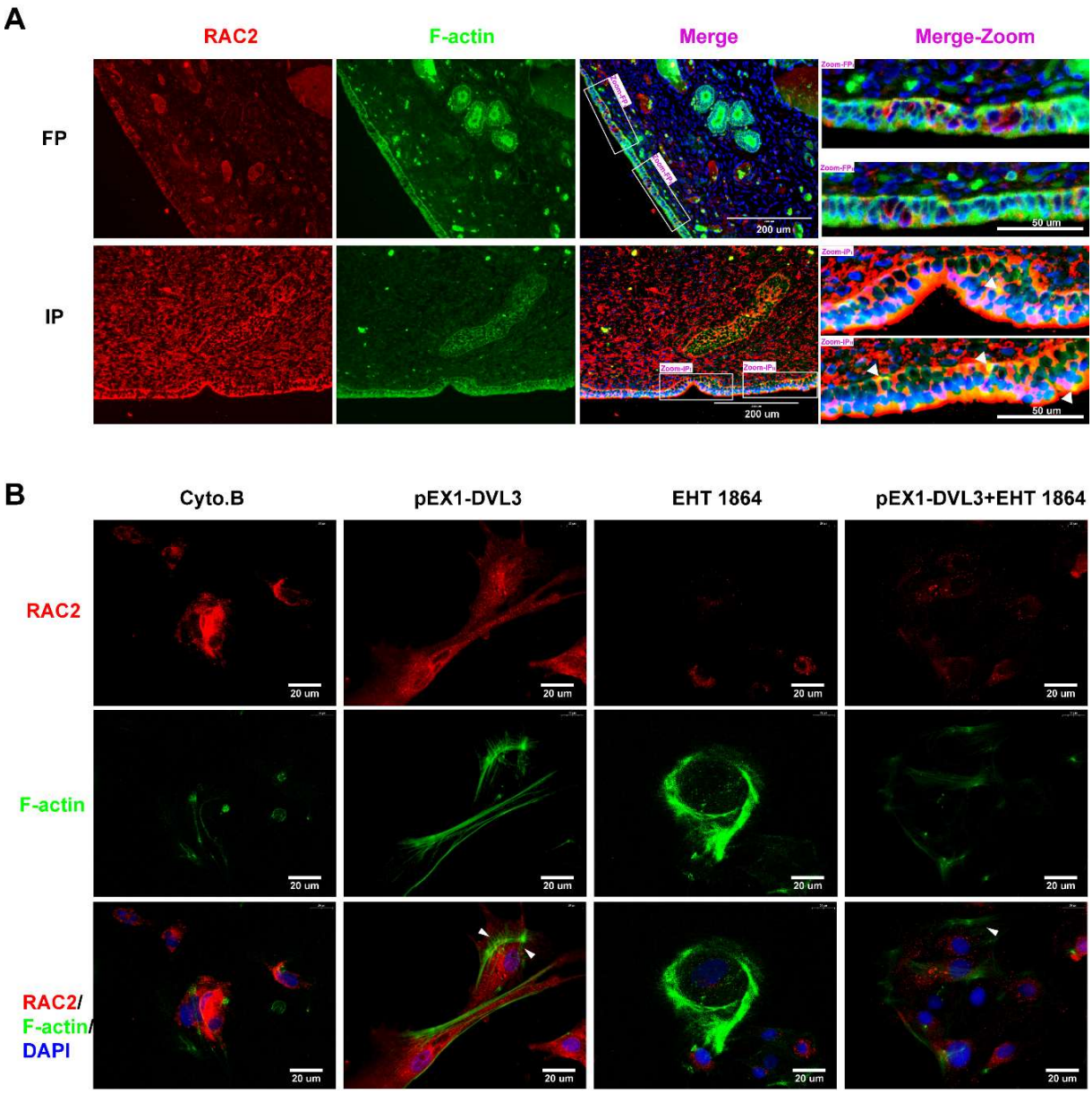

Fig. 7: Polymerization of filamentous actin is regulated by RAC2. (A) Expression and localization of RAC2 and F-actin in bovine endometrial tissues. (B) The effects of *DVL3* overexpression and/or RAC2 inhibition on the expression and localization of RAC2 and F-actin in bELECs.

(Grimm *et al.,* 2025; Oghbaei *et al.,* 2022). Thus, single-hormone exposure only alters microvilli height (Tran *et al.,* 2025). In contrast, our study reveals more complex changes in dairy cows during implantation. General histology and SEM showed flattened or smooth apical surfaces, surpassing the effects of individual hormones. This likely reflects ruminant placental specialization or IFN-τ signaling. These findings demonstrate that PMT requires coordinated hormonal and molecular signals(Lledo *et al.,* 2025; Whitby *et al.,* 2020a).

Another PMT hallmark is pinopode formation(Zhu *et al.,* 2025). First identified for their pinocytic function, these apical protrusions are now recognized as implantation markers across species. During PMT in endometrial luminal epithelium, actin polymerization and apical F-actin expression increase, contributing to the formation of pinopodes. The authors confirmed abundant mature pinopodes on bovine endometrial epithelia during implantation. Morphological analyses further showed intact membrane architecture, enabling pinocytic activity. Consequently, pinopodes serve as clinical indicators of endometrial receptivity(Kumro *et al.,* 2020; Zhou *et al.,* 2025), with proven utility in reproductive medicine.

The basolateral membrane of endometrial luminal epithelial cells is primarily composed of intercellular junctions. These junctions confer the unique apical-basal polarity characteristic of epithelial cells (Kumro *et al.,* 2020; Oghbaei *et al.,* 2022) (Whitby *et al.,* 2020a). Our study reveals that bovine endometrial luminal epithelium loses cellular polarity during the peri- and post-implantation periods compared to pre-implantation. The lateral plasma membrane shows structural disruption, indicating compromised intercellular junctions. During the peri-implantation window, tight junctions and desmosomes

in the lateral membrane undergo remodeling. This coincides with incomplete apical connections and reduced adhesive capacity. Notably, we observed downregulation of MUC1 at both transcriptional and protein levels in receptive bovine endometrium. This contrasts with human studies showing MUC1 upregulation in receptive endometrium, where it contributes to idiopathic infertility (Whitby *et al.,* 2020a) (Wang *et al.,* 2025). However, our findings align with reports demonstrating local MUC1 suppression at embryo implantation sites. Furthermore, integrin ITGB3 and N-cadherin were upregulated in receptive bovine endometrium. Concurrently, E-cadherin decreased while N-cadherin became detectable in luminal epithelial cells during implantation. Given that PMT shares the epithelial-to-mesenchymal transition phenotype with epithelial mesenchymal transition, their detection markers partially overlap. This study employed E-cadherin, N-cadherin, and CK18 as markers to evaluate PMT. This expression shift supports an epithelial-to-mesenchymal transition like process, facilitating trophoblast invasion and embryo implantation.

The evolutionary conservation of plasma membrane transformation implies regulation by conserved molecular pathways (Martins *et al.,* 2022b; Whitby *et al.,* 2020a; Zhang *et al.,* 2021). Mammalian pregnancy establishment requires coordinated steroid hormone and cytokine signaling. In ruminants, IFN-τ sustains corpus luteum function by modulating estrogen receptor activity and oxytocin signaling (Ma *et al.,* 2024). This study elucidates IFN-τ-mediated PMT regulation. Transcriptomic analysis revealed IFN-τ-induced differential genes enriched in pathways governing cell adhesion molecules, tight junctions, and cytoskeletal reorganization. We confirmed IFN-τ triggers cytoskeletal changes in bovine endometrial epithelial cells, facilitating PMT. IFN-τ upregulates the expression of DVL3 and RAC2 in both bovine endometrial tissue and bELECs. DVL3, a core component of the canonical Wnt/β-catenin pathway, also regulates downstream small GTPases to mediate cytoskeletal reorganization. Previous studies indicate that the small GTPases RhoA and RAC1 participate in murine embryo implantation, with RAC1 deficiency impairing uterine receptivity and leading to implantation failure by disrupting PMT. Moreover, the non-canonical Wnt/planar cell polarity (PCP) pathway plays a critical role in directing the oriented movement of endometrial epithelial cells during implantation cavity formation and the establishment of uterine receptivity. RAC2, a member of the small GTPase family, acts as a regulatory protein within the Wnt/PCP pathway. Cytoskeletal proteins provide the structural basis for increased contractility and actin stress fiber formation during epithelial-mesenchymal transition. Collectively, the Wnt/β-catenin and Wnt/PCP pathways, along with small GTPases and F-actin, exert essential regulatory functions in PMT. This study confirms a direct interaction between DVL3 and RAC2 through co-immunoprecipitation, co-localization by immunofluorescence, and western blot. Furthermore, overexpression and knockdown experiments demonstrate that RAC2 acts as a downstream effector of DVL3 in regulating PMT. Functional assays reveal that DVL3 promotes bELECs migration and reduces adhesion via RAC2, thereby maintaining normal PMT progression. RAC2 supports endometrial receptivity by facilitating actin polymerization. Notably, IFN-τ did not induce invasive behavior in bELECs, reflecting either fundamental differences between simplified in vitro systems and multifactorial in vivo regulation, or intrinsic distinctions between physiological implantation and malignant invasion processes (Guo *et al.,* 2025; Oghbaei *et al.,* 2022; Whitby *et al.,* 2020a). Collectively, these findings highlight the precise regulatory specificity inherent to reproductive systems.

Adhesion of cells to neighboring cells and the underlying extracellular matrix (ECM) constitutes a fundamental requirement for the survival of multicellular organisms. Consequently, the formation, stabilization, and dissociation of cellular adhesions are tightly spatiotemporally regulated, and perturbations in this sophisticated adhesive machinery are associated with various pathologies. Based on this rationale, the present study employed a real-time, label-free cellular analysis system to monitor cell-ECM adhesion dynamics. This approach is suitable for evaluating alterations in cellular adhesion induced by genetic manipulations, overexpression of proteins of interest, or drug treatments. We quantitatively assessed the effects of IFN-τ or DVL3 on the adhesive capacity of bovine endometrial epithelial cells. The technology utilizes electrode-integrated culture plates to monitor cellular impedance in real-time (Wei *et al.,* 2025), with impedance values directly correlating with tight junction integrity (Whitby *et al.,* 2020a). Cellular adhesion is represented by real-time changes in the mean cell index. Time point 0 denotes the initial scanning of the E-plate 96 following cell addition, while initial background scanning prior to cell seeding was excluded from analysis. Statistical analysis of endpoint cell index values between datasets was performed using GraphPad Prism and the Student's t-test. Our findings demonstrate that IFN-τ treatment alone, as well as combined DVL3 overexpression, significantly reduced the cell index. Comparative analysis between groups confirmed that DVL3 overexpression further augmented the IFN-τ-mediated reduction in cellular adhesive capacity, suggesting a potential role in pregnancy maintenance mechanisms. This methodology eliminates the requirement for embryo collection inherent in conventional spheroid adhesion assays and minimizes confounding embryonic signals, thereby significantly enhancing the accuracy of evaluating specific factors influencing endometrial adhesion. Furthermore, it expands the in vitro methodological framework for studying pregnancy establishment mechanisms.

Endometrial receptivity remains a central focus in reproduction. While significant progress has been made in understanding endometrial-embryo crosstalk, current diagnostic tools still lack sufficient accuracy in predicting receptivity (Doyle *et al.,* 2022). This limitation significantly contributes to the low success rates of assisted reproductive technologies. Substantial evidence demonstrates that peri-implantation endometrial changes, including physiological events, morphological transformations, and gene expression alterations, are prerequisites for receptivity establishment (Doyle *et al.,* 2022; Ma *et al.,* 2024; Zhang *et al.,* 2021; Zhou *et al.,* 2025). These coordinated changes create an optimal microenvironment for successful embryo implantation. However, endometrial receptivity involves complex

regulatory networks that cannot be adequately assessed through single molecular markers. Our study identifies PMT as a critical cellular event during endometrial receptivity establishment. We propose that systematic PMT monitoring could serve as a novel functional biomarker to complement existing molecular diagnostic approaches. Future research should integrate ultrastructural and biophysical PMT parameters with transcriptomic and proteomic analyses (Oghbaei *et al.,* 2022; Voros *et al.,* 2025). Such multidimensional assessment models could significantly improve reproductive health outcomes for both humans and animals by providing more comprehensive receptivity evaluation. This integrated approach may offer new theoretical foundations for enhancing fertility treatments.

Conclusions: This study elucidates that IFN-τ orchestrates plasma membrane transformation in bovine endometrial luminal epithelial cells via the DVL3/RAC2 signaling pathway, a critical mechanism underpinning endometrial receptivity during peri-implantation. The findings highlight IFN-τ's dual role in disrupting intercellular junctions to promote cellular plasticity and enhancing cytoskeletal dynamics through RAC2-mediated actin polymerization, collectively fostering a receptive endometrial microenvironment. These insights position IFN-τ as a promising therapeutic candidate for addressing implantation failure linked to aberrant endometrial receptivity.

Authors contribution: Xiaofei Ma: Writing –original draft, Writing – review & editing, Investigation, Data curation, Conceptualization, Funding acquisition. Zhonghong Bai: Methodology, Investigation. Tingting Liu: Data curation, Resources, Supervision. Saqib Umer: Writing – review & editing. Junjie Hu: Writing – review & editing. Ganzhen Deng: Supervision, Funding acquisition, Conceptualization, Project administration, Resources.

Declaration of competing interest: The authors have declared that no competing interest exists or personal relationships.

Acknowledgements: This research was supported by the fund of the College of Veterinary Medicine of Gansu Agricultural University (GSAU-CVM), Doctoral Research Startup Project of Gansu Agricultural University (GAU-KYQD-2022-33), the Natural Science Foundation of Gansu Science and Technology Plan (NO.23JRRA1411), and the University Teachers Innovation Fund of Gansu Department of Education (2024B-080), and National Natural Science Foundation of China (NO. 31972744).

We gratefully acknowledge the technical support from all members of the Gansu Key Laboratory of Animal Generational Physiology and Reproductive Regulation. We particularly thank Prof. Ganzhen Deng (Department of Clinical Veterinary Medicine, Huazhong Agricultural University) for providing access to transmission electron microscopy, scanning electron microscopy, and RTCA-DP instrumentation. The schematic illustrations were created using BioRender.com. We would like to thank Editage (www.editage.cn) for English language editing.

REFERENCES

Baron C, Haouzi D, Gala A, *et al*., 2021. Endometrial receptivity in assisted reproductive techniques: An aspect to investigate in embryo implantation failure. Gynécologie Obstétrique Fertilité & Sénologie. 49: 128-136.

Borday C, Parain K, Thi Tran H, *et al*., 2018. An atlas of Wnt activity during embryogenesis in Xenopus tropicalis. PLoS One. 13: e0193606.

Dimova T, Alexandrova M, Vangelov I, *et al*., 2025. The modeling of human implantation and early placentation: achievements and perspectives. Human Reproduction Update. 31: 133-163.

Doyle N, Jahandideh S, Hill MJ, *et al*., 2022. Effect of Timing by Endometrial Receptivity Testing vs Standard Timing of Frozen Embryo Transfer on Live Birth in Patients Undergoing In Vitro Fertilization: A Randomized Clinical Trial. Jama. 328: 2117-2125.

Dudley JS, Murphy CR, Thompson MB, *et al*., 2018. Uterine Epithelial Cells Undergo a Plasma Membrane Transformation During Early Pregnancy in the Domestic Cat (Felis catus). Anatomical Record (Hoboken). 301: 1497-1505.

Grimm TM, Dierdorf NI, Herbinger M, *et al*., 2025. The phosphatase PPM1F, a negative regulator of integrin activity, is essential for embryonic development and controls tumor cell invasion. BMC Biology. 23: 166.

Guo W, Duan Z, Wu J, *et al*., 2025. Epithelial-mesenchymal transition promotes metabolic reprogramming to suppress ferroptosis. Semin Cancer Biology. 112: 20-35.

Jin P, Cai J, Chen N, *et al*., 2025. TGF-β/snail-mediated epithelial-to-mesenchymal transition disrupts estradiol metabolism through suppressing the HSD17B2 expression in endometriotic epithelial cells. Biochemistry Biophysics Research Communication. 771: 151964.

Kumro FG, O'Neil EV, Ciernia LA, *et al*., 2020. Scanning electron microscopy of the surface epithelium of the bovine endometrium. Journal of Dairy Science. 103: 12083-12090.

Liu W, Chen J, Yang C, *et al*., 2022. Expression of microRNA let-7 in cleavage embryos modulates cell fate determination and formation of mouse blastocysts†. Biology Reproduction. 107: 1452-1463.

Lledo B, Hortal M, Martínez M, *et al*., 2025. Association of estrogen and progesterone receptor polymorphisms with idiopathic thin endometrium. Pharmacogenetic Genomics. 35: 136-139.

Ma B, Cui H, Wang X, *et al*., 2024. IFNT-induced IRF1 enhances bovine endometrial receptivity by transactivating LIFR, Journal of Reproduction Immunology. 163:104212.

Ma X, Yin B, Guo S, *et al*., 2021. Enhanced Expression of miR-34a Enhances Escherichia coli Lipopolysaccharide-Mediated Endometritis by Targeting LGR4 to Activate the NF-kappaB Pathway, Oxidative Medicine Cell Longevity. 2021: 1744754.

Martins T, Sponchiado M, Silva F, *et al*., 2022a. Progesterone-dependent and progesterone-independent modulation of luminal epithelial transcription to support pregnancy in cattle, Physiology Genomics. 54: 71-85.

Martins T, Sponchiado M, Silva FACC, *et al*., 2022b. Progesterone-dependent and progesterone-independent modulation of luminal epithelial transcription to support pregnancy in cattle, Physiologicy Genomics. 54: 71-85.

Maurice MM, Angers S, *et al*., 2025. Mechanistic insights into Wnt-β-catenin pathway activation and signal transduction, Nature Reviews Molecular Cell Biology. 26: 371-388.

Murphy CR, Shaw TJ, *et al*., 2004. Uterine receptivity and the plasma membrane transformation, Cell Research. 14: 259-267.

Murphy CR, Shaw TJ, *et al*., 1994. Plasma membrane transformation: a common response of uterine epithelial cells during the peri-implantation period, Cell Biology International. 18: 1115-1128.

Oghbaei F, Zarezadeh R, Jafari-Gharabaghlou D, *et al*., 2022. Epithelial-mesenchymal transition process during embryo implantation, Cell Tissue Research. 388: 1-17.

Owusu-Akyaw A, Krishnamoorthy K, Goldsmith LT, *et al*., 2019. The role of mesenchymal-epithelial transition in endometrial function, Human Reproduction Update. 25: 114-133.

Rodriguez-Alonso B, Sanchez JM, Hamdi M, *et al*., 2020. Asynchrony between the early embryo and the reproductive tract affects subsequent embryo development in cattle, Reproduction Fertility Development. 32: 564-571.

Rodríguez-Eguren A, Bueno-Fernandez C, Gómez-Álvarez M, *et al*., 2024. Evolution of biotechnological advances and regenerative therapies for endometrial disorders: a systematic review, Human Reproduction Update. 30: 584-613.

Schmiech K, Li M, Chen LX, *et al*., 2025. Association of endometrial thickness with live birth rate: a study using the Society for Assisted Reproductive Technology Clinic Outcome Reporting System, Fertility Sterility. 124: 79-87.

Shang J, Chen Y, Jiang Q, *et al*., 2025. The long noncoding RNA LUCAT1 regulates endometrial receptivity via the miR-495-3p/S100P axis, Communication Biology. 8: 318.

Shibata S, Endo S, Nagai LAE, *et al*., 2024. Modeling embryo-endometrial interface recapitulating human embryo implantation, Science Adventure. 10: eadi4819.

Tran DN, Hwang YJ, Kim KC, *et al*., 2025. GRB2 regulation of essential signaling pathways in the endometrium is critical for implantation and decidualization, Nature Communication. 16: 2192.

Voros C, Varthaliti A, Athanasiou D, *et al*., 2025. MicroRNA Signatures in Endometrial Receptivity-Unlocking Their Role in Embryo Implantation and IVF Success: A Systematic Review, Biomedicines. 13.

Wang H, Chen K, Zong L, *et al*., 2024. MALAT1/miR-7-5p/TCF4 Axis Regulating Menstrual Blood Mesenchymal Stem Cells Improve Thin Endometrium Fertility by the Wnt Signaling Pathway, Cell Transplant. 33: 9636897241259552.

Wang X, Li M, Han J, *et al*., 2025. Estrogen-Regulated Proline-Rich Acidic Protein 1 in Endometrial Epithelial Cells Affects Embryo Implantation by Regulating Mucin 1 in Mice, Biomolecules. 15.

Wango EO, Wooding FB, Heap RB, *et al*., 1990. The role of trophoblastic binucleate cells in implantation in the goat: a morphological study, Journal Anatomy. 171: 241-257.

Wei Z, Babkirk K, Chen S, *et al*., 2025. Epithelial-to-mesenchymal transition transcription factors: New strategies for mesenchymal tissue regeneration, Cytokine Growth Factor Reviews. 83: 99-124.

Whitby S, Zhou W, Dimitriadis E, *et al*., 2020a. Alterations in Epithelial Cell Polarity During Endometrial Receptivity: A Systematic Review, Front Endocrinol (Lausanne). 11: 596324.

Whitby ST, Zhou W, Dimitriadis E, *et al*., 2020b. Alterations in Epithelial Cell Polarity During Endometrial Receptivity: A Systematic Review, Frontiers in Endocrinology. 11.

Wiltbank MC, Monteiro PLJ, Domingues RR, *et al*., 2023. Review: Maintenance of the ruminant corpus luteum during pregnancy: interferon-tau and beyond, Animal 17 Suppl. 1: 100827.

Yang MK, Yeh RH, Lee CJ, *et al*., 2024. Pregnancy maintenance and fetal loss assessment in Holstein cows through analyzing pregnancy-associated glycoproteins in milk, Theriogenology. 217: 11-17.

Zhang T, Guo S, Zhou H, *et al*., 2021. Endometrial extracellular matrix rigidity and IFN tau ensure the establishment of early pregnancy through activation of YAP, Cell Proliferation. 54.

Zhao G, Jiang K, Zhang T, *et al*., 2018. Specific interferon tau gene-regulation networks in bovine endometrial luminal epithelial cells, Theriogenology. 105: 51-60.

Zhou H, Zhang J, Feng W, *et al*., 2025. YAP1 regulates endometrial receptivity by promoting the plasma membrane transformation and proliferation of bovine endometrial epithelial cells, Theriogenology. 237:166-177.

Zhu MB, Chen BL, Cen M, *et al*., 2025. Comparative analysis of endometrial gland imaging and pinopode detection for assessing endometrial receptivity, Reproduction Biology Endocrinology. 23: 62.